UC Irvine
UC Irvine Previously Published Works

Title

Bias Adjustment of Satellite Precipitation Estimation Using Ground-Based Measurement: A Case Study Evaluation over the Southwestern United States

Permalink

https://escholarship.org/uc/item/5qb317c4

Journal

Journal of Hydrometeorology, 10(5)

ISSN

1525-755X

Authors

Boushaki, Farid Ishak
Hsu, Kuo-Lin
Sorooshian, Soroosh
et al.

Publication Date

2009-10-01

DOI

10.1175/2009jhm1099.1

Copyright Information

Peer reviewed

Bias Adjustment of Satellite Precipitation Estimation Using Ground-Based Measurement: A Case Study Evaluation over the Southwestern United States

FARID ISHAK BOUSHAKI, KUO-LIN HSU, SOROOSH SOROOSHIAN, AND GI-HYEON PARK

*Center for Hydrometeorology and Remote Sensing, Department of Civil and Environmental Engineering,
University of California, Irvine, Irvine, California*

SHAYESTEH MAHANI

*NOAA/CREST Center, Civil Engineering Department, City College of New York, City University of New York,
New York, New York*

WEI SHI

NOAA/Climate Prediction Center, Camp Springs, Maryland

ABSTRACT

Reliable precipitation measurement is a crucial component in hydrologic studies. Although satellite-based observation is able to provide spatial and temporal distribution of precipitation, the measurements tend to show systematic bias. This paper introduces a grid-based precipitation merging procedure in which satellite estimates from the Precipitation Estimation from Remotely Sensed Information using Artificial Neural Networks–Cloud Classification System (PERSIANN–CCS) are adjusted based on the Climate Prediction Center (CPC) daily rain gauge analysis. To remove the bias, the hourly CCS estimates were spatially and temporally accumulated to the daily $1° \times 1°$ scale, the resolution of CPC rain gauge analysis. The daily CCS bias was then downscaled to the hourly temporal scale to correct hourly CCS estimates. The bias corrected CCS estimates are called the adjusted CCS (CCSA) product. With the adjustment from the gauge measurement, CCSA data have been generated to provide more reliable high temporal/spatial-resolution precipitation estimates. In the case study, the CCSA precipitation estimates from the proposed approach are compared against ground-based measurements in high-density gauge networks located in the southwestern United States.

1. Introduction

Accurate estimation of precipitation is crucial to a range of hydrologic and climatic applications. These applications vary from flood forecasting to climatological studies of droughts. At present, there are several precipitation measurement systems, including point measurements at gauge and spatial measurements from radar and satellite. Although gauges are considered to be the only source of physical measurement, the lack of temporal and spatial sampling hinders the relevance of such measurement. To overcome such a problem, recent developments in re-mote sensing technology (satellite and radar) provide potential alternatives for high spatial/temporal estimates of precipitation, especially in semiarid regions where ground measurements are lacking or sparse at best. Although weather radar provides precipitation estimates at high spatial/temporal resolution, its performance does not account for evaporation loss and is grossly inadequate over the mountainous regions as a result of beam blockage, especially in the southwestern United States where precipitation contributes to most of the water supply.

Advancement in satellite information technology has grown tremendously in the last two decades. These advances triggered the atmospheric community and, to some extent, the hydrologic community to develop algorithms aimed at retrieving precipitation data from cloud information. Although satellite precipitation has

Corresponding author address: Kuo-Lin Hsu, Civil and Environmental Engineering, University of California, Irvine, 34130 Engineering Gateway, Irvine, CA 92697-2175.
E-mail: kuolinh@uci.edu

been widely used in meteorological models, because of its large-scale approach, especially in the area of limited access to ground-based measurements, the hydrologic community is also interested in using satellite precipitation data for both research and application purposes. The National Weather Service (NWS), for example, is using satellite data in an effort to improve flash-flood watches and warnings and heavy precipitation forecasts (Vicente et al. 1998).

The approach of estimating precipitation amounts from satellite imagery infers the rate of precipitation from the characteristics of clouds in infrared, visible, and microwave satellite images. Such an approach offers some significant advantages compared to rain gauge and radar estimates. Satellite data provide uniform spatial coverage, whereas the poor spatial resolution of rain gauge data makes it difficult to accurately represent the spatial variability of precipitation fields. Furthermore, satellites offer excellent coverage over mountainous areas compared to radar observations. The Tropical Rainfall Measuring Mission (TRMM) is a newer generation of satellite precipitation estimates that introduces the precipitation radar instrument (active microwave) and the TRMM microwave imager [passive microwave (PMW)] for rainfall estimation (Kummerow et al. 1998).

For the spatial and temporal consideration, geosynchronous orbit (GEO) satellites can provide less-than-hourly samples and are frequently used to monitor cloud motion and provide information that indirectly infers rainfall at the ground surface. This gives rise to the uncertainty of retrieval. On the other hand, PMW sensors carried by low earth orbit (LEO) satellites can sense rainy clouds more directly. However, the hind side is that each LEO satellite provides limited temporal samples and lower spatial coverage. To use the strengths and compensate the weaknesses of those PMW and IR sensors, algorithms were developed to jointly use GEO and LEO satellite information. The results demonstrated the great potential of improving surface rainfall retrieval (Adler et al. 1993; Ba and Gruber 2001; Bellerby et al. 2000; Hong et al. 2004; Hsu et al. 1997, 1999; Huffman 1997; Huffman et al. 2001; Joyce et al. 2004; Levizzani et al. 2007; Marzano et al. 2004; Sorooshian et al. 2000; Tapiador et al. 2004; Turk et al. 2000; Vicente et al. 1998; Xie and Arkin 1997).

Because blending approaches using LEO and GEO satellite information may provide potential improvement than using one single source, without referencing to the ground measurement, those precipitation estimates may be biased from surface rainfall, either regionally or temporally. Additional measurement from gauges helps to reduce bias from satellite measurement. Although improvement has been made from merging satellite and gauge measurements at monthly scale or even for providing adjustment at daily scale based on global monthly gauge measurement (Xie and Arkin 1997; Huffman et al. 2001), a finescale precipitation measurement at subdaily scale is needed for many hydrologic applications. We intend to address this issue by downscaling daily gauge measurement from daily 0.25° resolution to subdaily 0.04° scale using hourly precipitation estimation from multiple satellites.

In this study, given the challenge of improving the reliability of high-resolution, large-extent rainfall maps based on satellite observation over land, we introduce a grid-based merging procedure in which satellite estimates from the Precipitation Estimation from Remotely Sensed Information using Artificial Neural Networks–Cloud Classification System (PERSIANN–CCS) are integrated with a grid-based ground measurement source known as the Climate Prediction Center (CPC) daily rain gauge analysis to produce a satellite–gauge bias-adjusted precipitation product called PERSIANN–CCSA (CCSA). Multiple years of over-land precipitation data were generated from 2001 until 2006. These data can potentially be used as a forcing variable to the hydrologic modeling, studying climate variation through land cover changes and supporting water resources management and decision making. These precipitation products cover from −135° to −65° longitude, and 10°–50° latitude at 0.04° spatial resolution and hourly temporal resolution. The resulting rainfall estimates from the CCSA are compared and validated against ground-based rainfall observations over several locations in the southwestern United States.

2. Precipitation measurement

Variability of rainfall has been acknowledged as a reason for the uncertainties in hydrologic applications (Droegemeier et al. 2000). This inherent problem requires new methodologies to improve the reliability of the current precipitation products by combining precipitation information from different sources. Conventional ground-based rain gauges are the most common rain sensors in use that directly measure precipitation falling on the ground, but they are not able to picture the spatial pattern of rainfall (Huff 1970). Another precipitation measurement system is the weather radar that is based on converting radar reflectivity Z to rain rate R through the $Z–R$ relationship and provides precipitation estimates at high spatial/temporal resolution (Marshall et al. 1948; Battan 1973; Morin et all. 2005). The third potentially useful measurement system is the satellite precipitation estimates. It is based upon the analysis of clouds by combining geostationary satellite information with low orbiting satellites data, resulting in a precipitation

rate with high spatial/temporal resolution. A brief discussion of the strengths and weaknesses of each precipitation source is listed below.

Gauge observations sample only some points over the watershed. To obtain the mean areal precipitation (MAP), we assume a spatial geometry tied to point rain gauge observations using, for example, Thiessen polygons, inverse distance-squared weighting, or statistical Kriging techniques. Unfortunately, these estimates of rainfall could have large errors that might be propagated directly into streamflow estimation. In addition, rain gauge measurements are subject to a variety of error sources. Globally, gauge measurements tend to underestimate precipitation because of wind-induced turbulence at the gauge orifice, wetting losses on gauge walls, splashing, and evaporation (Legates 1993). Monthly biases in rain gauge measurements are thought to range between 5% and 40%, with the largest errors occurring during snowfall (Groisman and Easterling 1994). Although Sevruk (1985) states that systematic gauge errors are the most significant source of error, representativeness errors can also be quite large. Representativeness errors occur in two forms. The first is associated with individual gauges: the amount of precipitation measured at a gauge may not adequately represent the rainfall amount in its vicinity because of localized climatological variations. The second is associated with the gauge network as a whole: if the network is not dense enough to completely describe the spatial variability of a precipitation field, assumptions must be made about the amount and timing of precipitation in those locations with no gauge coverage, and these assumptions can be significant sources of error.

Radar measurements, on the other hand, augment gauge measurements to provide detailed spatial- and temporal-resolution measurement of precipitation over an extensive spatial domain. Surface-based weather radar emits electromagnetic energy at wavelengths that are sensitive to the distribution of water droplets in air. The radar reflectivity, as a function of the measured reflected power, is related to the precipitation intensity at ground level in the corresponding region. The latter is estimated empirically by the so-called $Z–R$ relationship. Sources of errors in radar measurement, as summarized by Wilson and Brandes (1979), including the following: 1) the $Z–R$ relationship, which varies from radar to radar and from storm type to storm type; 2) melting snow, which reflects much more energy than raindrops and produces anomalously high returns (brightband); and (3) that as the height of the radar beam increases, the difference in precipitation rate between the radar scan level and the ground becomes greater (i.e., evaporation difference), in addition to beam blockage by mountains, which restricts radar observations.

Satellites offer better coverage than radar observations and gauges, especially in mountainous regions. Satellite-based rain retrievals either use information from the visible and infrared spectral channels of GEO satellites to establish an indirect relationship between surface rainfall rate and the observed characteristics of the cloud features, or from passive/active microwave spectral channels of low orbiting satellites to detect rainfall rate by their capability of sensing the hydrometeor distribution of the clouds. However, samples from microwave measurements are less frequent (e.g., twice a day). Similar to radar, a satellite observes the cloud thermal radiance instead of directly measuring rainfall, creating rainfall estimation errors. Although satellite measurement covers a larger spatial domain than gauge network, cold nonprecipitating clouds and warm precipitating clouds are easily miscalculated.

3. Merging satellite and gauge precipitation observations

a. Data used

Two sources of data are used in this study to produce biased-corrected satellite precipitation estimates. Satellite-based rainfall is provided from the Center for Hydrometeorology and Remote Sensing, University of California, Irvine (CHRS UCI), and daily gauge rainfall is available from the National Oceanic and Atmospheric Administration (NOAA)/CPC. These two data sources are described next.

1) PERSIANN–CCS RAINFALL DATA

The satellite precipitation product used is entitled PERSIANN–CCS (Hong et al. 2004). The PERSIANN–CCS uses computer image processing and pattern recognition techniques to develop a patch-based cloud classification that estimates rainfall at higher spatial and temporal resolution. This algorithm segments the longwave infrared cloud image, assigns rainfall distribution to the patch image, and then calculates pixel rainfall intensity based on a classification-based artificial neural network model. The PERSIANN–CCS system produces hourly estimates at the spatial resolution of $0.04° \times 0.04°$ that can be applied to the basin-scale hydrologic applications. CCS estimates over the conterminous United States (CONUS) are provided by CHRS of UCI (available online at http://hydis8.eng.uci.edu/CCS/).

2) NOAA/CPC DAILY ANALYSIS

The CPC has developed a grid-based quality-controlled gauge precipitation system that supports climate monitoring and applied research. This system was built in
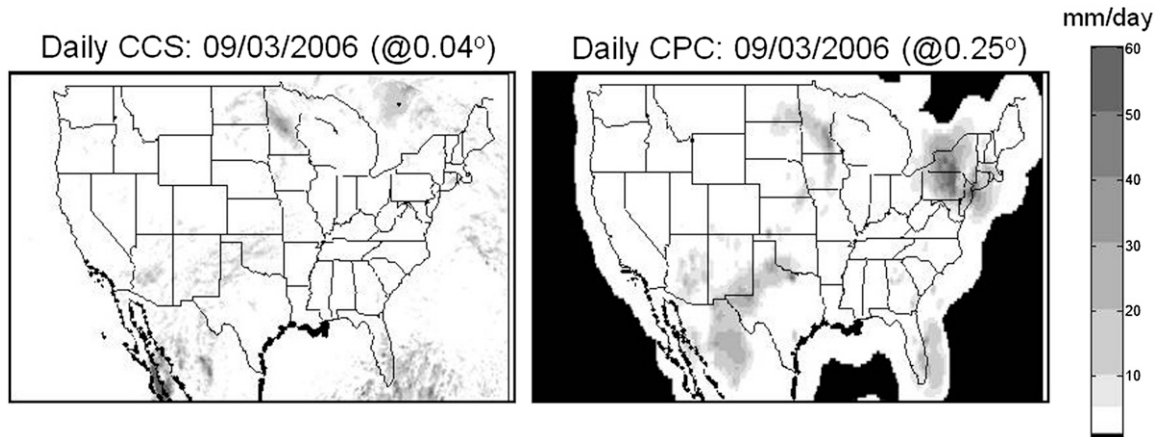
FIG. 1. Example of the daily CCS precipitation image vs the daily CPC.

1997 and has been undergoing continuous development and improvement since then. This product is used for a variety of other products, such as the National Centers for Environmental Prediction (NCEP) regional reanalysis project and the U.S. Drought Forecast System (Higgins et al. 2000). This dataset consists of daily averaged precipitation rate values (mm day^{-1}) at 0.25° latitude/longitude resolution over the United States and Mexico that use available rain gauge datasets from different agencies. Figure 1 shows an example of the original daily PERSIANN–CCS image at 0.04° × 0.04° spatial resolution and the daily reference CPC image at 0.25° × 0.25°. (The daily CPC gauge precipitation product is available online at http://www.cpc.ncep.noaa.gov/products/precip/realtime/GIS/retro.shtml.) Additional information about the CPC analysis product can also be found at that Web site.

b. The merging methodology

The bias in satellite-based estimates originates from the fact that satellites remotely measure atmospheric characteristics and then infer precipitation estimates through different algorithms. Many researchers have been investigating this issue since the satellite-based precipitation estimates were made available in the 1970s (e.g., Scofield and Oliver 1977; Rosenfeld and Mintz 1988; Morrissey 1991; Smith and Krajewski 1991; Xie and Arkin 1997; Huffman 1997; Adler et al. 2000; Gruber et al. 2000; McCollum et al. 2000, 2002; Bowman et al. 2003; Smith et al. 2006). Bias-adjustment methods rely either on computing the difference between satellite- and gauge-based precipitation where gauge-based measurements are available or on a combination of several satellite-based estimates in regions with no gauges. Methods using gauge measurements are referred to as direct-bias estimates and include optimum interpolation

(Gandin 1963; Reynolds and Smith 1994), smart interpolation (Willmott and Matsuura 1995), and CPC merged analysis of precipitation (Xie and Arkin 1997).

The merging methodology followed in this work is similar to the approach described in Daley (1991). It is based on adjusting the differences between the daily gauge distribution and the satellite rainfall at and near the grid boxes and the inclusion of the number of gauges available at each pixel as a confidence; that is, the higher the number of gauges that exist within a pixel grid, the more weight is given to that pixel. It needs to be mentioned that the CPC gauge product is available at daily temporal resolution at 0.25° × 0.25° latitude–longitude resolution; therefore, the algorithm consists of a two-step process in which the daily adjustment at 0.25° × 0.25° is carried out first, followed by the hourly adjustment at 0.04° × 0.04° scale. The daily bias is calculated and removed from the satellite daily product on each pixel at 0.25° × 0.25° scale as follows:

$$\mathrm{Er}_D^k = \sum_{i \in \Omega_k} [w_i (G_D^i - P_{O(D)}^i)] \Big/ \sum_{i \in \Omega_k} w_i' \qquad (1)$$

where Er_D^k is the daily error of pixel k of the satellite-based rainfall (mm day^{-1}), G_D is the daily gauge-based rainfall at pixel k (mm day^{-1}), $P_{O(D)}$ is the daily satellite-based rainfall at pixel k (aggregated from hourly CCS and in mm day^{-1}), and Ω_k defines the neighborhood region centered at pixel k (0.25° × 0.25° grid). In this case, Ω_k is selected as 3 × 3 neighborhood pixels. Also, w_i is the weighting factor that is a function of gauge counts of pixel k and the inverse distance from pixel k to pixel i, which is defined as

$$w_i = w_{id} \times w_{ig}, \qquad (2)$$

where w_{id} is the inverse distance weighting factor from the center pixel k to pixel i and w_{ig} is the gauge density weighting factor at pixel k. They are defined as

$$w_{id} = \frac{(D^2 - d_i^2)}{(D^2 + d_i^2)} \quad \text{and} \tag{3}$$

$$w_{ig} = f(\text{GC}, \alpha, \varepsilon)$$

$$= \begin{cases} 0 \longrightarrow & \text{if} \quad (\text{GC} < \varepsilon) \\ \text{GC}/\alpha \longrightarrow & \text{if} \quad (\varepsilon < \text{GC} < \alpha) \\ 1 \longrightarrow & \text{if} \quad (\text{GC} > \alpha), \end{cases} \tag{4}$$

where D is the maximum distance from the center of pixel k to the center of the outer pixel window (in this case, a 3×3 window); d is the distance from the center pixel i to the center pixel k, respectively; GC is the gauge count, and α is the upper threshold of gauge counts (in this study, α is set to 20); and ε is the lower threshold of the number of gauges accepted within a pixel (here, ε is set to 4).

Note that the correction is completed by adjusting CCS estimates toward the daily CPC gauge product. This adjustment depends on the gauge counts and precipitation estimation at the calculation pixel and its neighborhood pixels. For example, if the calculation pixel k contains fewer than four gauges, then the weight w_i is assigned as zero; therefore, the daily adjustment mainly depends on the weighted adjustment of gauge and CCS difference of its neighborhood pixels [see Eqs. (1) and (2)]. If all 0.25° pixels in the neighborhood k contain gauge counts fewer than four, then no adjustment is given in the pixel k.

After calculating the daily bias for each pixel, it is then removed from the daily satellite rainfall estimate:

$$P_{A(D)}^j = P_{O(D)}^j + \frac{P_{O(D)}^j}{\sum_{j \in \Lambda_k} P_{O(D)}^j} [\text{Er}_{(D)}^k \times n(\Lambda_k)], \tag{5}$$

where k is an index defined in the CPC gauge product resolution (0.25° × 0.25°), Λ_k is the coverage of a CPC product grid, and j is an index for CCS grids at resolution 0.04° × 0.04° inside each CPC 0.25° × 0.25° grid. The grid j is defined as the subgrid of CPC product grid k, in which every pixel j is covered by a CPC data product grid k. Here, $P_{A(D)}^j$ is the adjusted daily rainfall at pixel j (mm day^{-1}), at 0.04° × 0.04° resolution; $P_{O(D)}^j$ is the CCS daily rainfall at pixel i (mm day^{-1}), at 0.04° × 0.04° resolution; and $n(\Lambda_k)$ is the number of CCS pixels under the coverage of a CPC gauge product grid, which includes about 6 × 6 CCS pixels.

After generating the daily product, the hourly adjusted rainfall is calculated by multiplying the CCS satellite-
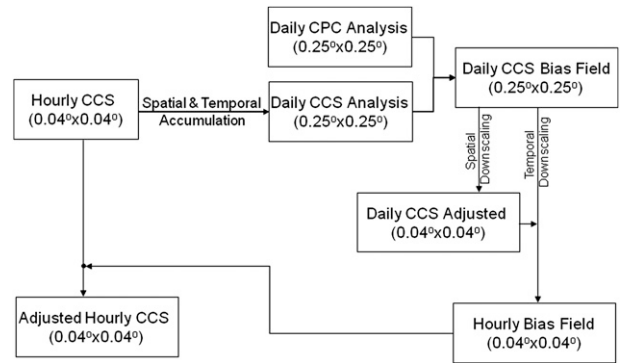

FIG. 2. The processing steps of adjusting hourly CCS rainfall data using daily CPC rainfall.

based hourly values at each grid point by the ratio of the daily adjusted product to the daily original CCS rainfall:

$$P_{A(h)}^k = P_{O(h)}^k \times \frac{P_{A(D)}^k}{P_{O(D)}^k}, \tag{6}$$

where h denotes the hourly resolution, D denotes the daily resolution, A represents the CCSA, and O represents the original CCS. This hourly adjustment is based on the assumption that a higher amount of precipitation holds higher error and vice versa. The process to generate the CCSA for each hour is shown in Fig. 2.

4. Product evaluation

a. Daily evaluation

The hydrometeorology of the southwestern United States semiarid region is characterized by intense thunderstorm episodes during the summer season that have a major contribution to the yearly total precipitation. The focus of the daily analysis is contained to the 3-month period of July–September (JAS) from 2002 to 2006 in the southwestern United States, where most of the precipitation occurs during this period (Gochis et al. 2006). We selected two regions (a 1° × 1° box) in Arizona (see Fig. 3a) for the daily analysis. Region 1 was chosen because it consists of a dense network of 91 gauges that are used in the CPC estimates (see Fig. 3b), whereas region 2 has only 8 gauges over the 1° × 1° box. This contrast analysis will show the performance of the merging process in converging CCS rainfall satellite-based estimation to CPC ground measurements for high and low gauge count areas over the southwestern United States. Figure 4 shows the scatterplots of the daily CCS and CCSA to the CPC daily analysis over the two regions. Quantitatively, the accuracy of estimates is evaluated
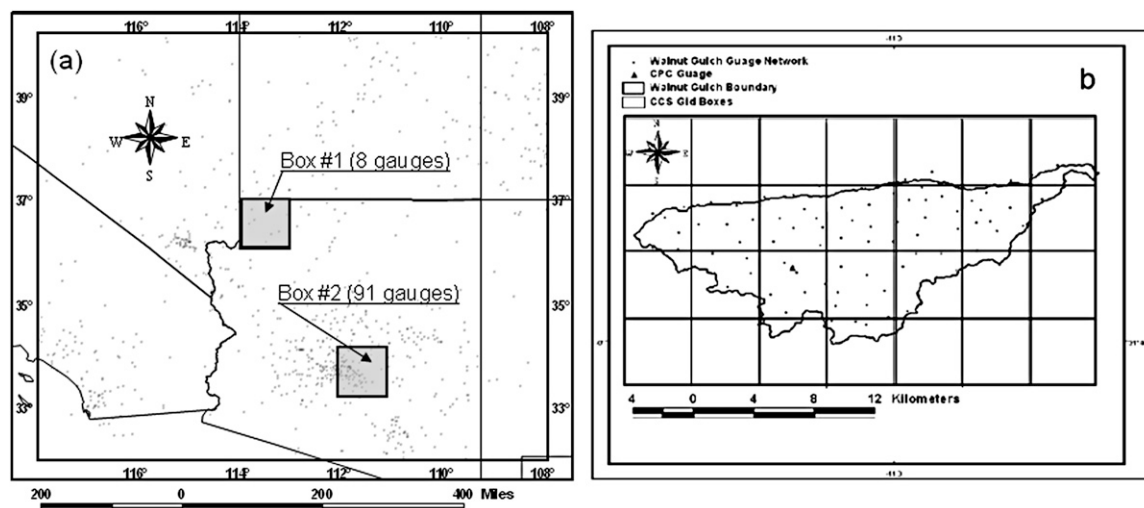
FIG. 3. Location of the study area in the southwestern United States. (a) The evaluation study locations (regions 1 and 2) and their CPC gauge distribution. (b) Location of the Walnut Gulch watershed with the ARS high-gauge network distribution.

using the correlation coefficient (R, or Corr), the mean bias (BIAS), and the root-mean-square error (RMSE):

$$\text{RMSE} = \left\{ \frac{1}{n} \sum_{t=1}^{n} [P_g(t) - P_s(t)]^2 \right\}^{0.5} \qquad (7)$$

$$\text{BIAS} = \frac{1}{n} \sum_{t=1}^{n} [P_g(t) - P_s(t)], \quad \text{and} \qquad (8)$$

$$R = \frac{\sum_{t=1}^{n} P_g(t)P_s(t) - (n\overline{P}_g\overline{P}_s)}{\sqrt{\left[\sum_{t=1}^{n} P_g(t)^2 - n\overline{P}_g^2\right]\left[\sum_{t=1}^{n} P_s(t)^2 - n\overline{P}_s^2\right]}}, \qquad (9)$$

where $P_g(t)$ represents the reference ground measurements, $P_s(t)$ is the satellite estimates (CCS or CCSA) at time t, $\overline{P}_g$ and $\overline{P}_s$ are the mean average of each, and n is the number of data points.

The scatterplots in Fig. 4 illustrates the improvement of the satellite estimates after the bias adjustment procedure, considering the CPC gauge analysis as a reference. These plots also show a same general trend of rainfall overestimation from original satellite estimates in summer seasons as reported by other studies (Yilmaz et al. 2005). Originally, the CCS overestimates the rainfall over region 1 (see Fig. 4a), resulting in a correlation coefficient of 0.64, a BIAS of 1.02 mm d^{-1}, and an RMSE of 3.71 mm d^{-1}. When the bias adjustment procedure is applied to the original CCS data (see Fig. 4b), the overestimation of the new CCSA to the CPC is decreased, resulting in a higher correlation coefficient of

0.96, and a reduction of the bias and RMSE (0.04 and 0.69 mm d^{-1}, respectively). Similar results are observed for the lower gauge count region (see Figs. 4c,d), in which the correlation improved from 0.65 to 0.95, the BIAS reduced from 0.89 to 0.17 mm d^{-1}, and the RMSE reduced from 3.14 to 0.56 mm d^{-1}. Results of this daily cross testing shows that the overestimated bias by satellite can be tremendously reduced using the bias adjustment procedure presented herein when relying on the CPC gauge analysis as a reference. The time series of the daily precipitation show an agreement between the CPC and CCS in terms of detecting rainfall events; however, a considerable variation in the bias is noticed along the time series over the two regions. During the JAS season of 2006, for example (Fig. 5a), a significant positive bias starts from July over region 1 that continues to manifest itself with lower magnitude during August, and becomes slightly negative by the end of August to the end of September. Similar to region 1, region 2 (Fig. 5b) shows an overall positive bias during July and August and then becomes a negative bias during the 4-day period of 7–10 July and the month of September. The CCSA, however, shows a very good agreement with the CPC, in which the bias-adjusted procedure was able to correct for the negative and positive biases alternatively. It is important to carry out this study to a watershed level and higher temporal resolution to evaluate the significance of satellite data for hydrologic applications in which such resolution is needed.

b. Hourly evaluation

Although the daily CCSA shows improvement over the daily CPC gauge analysis, it is useful to show the

Region #1: Daily Rainfall (July, August, and September: 2002-2006)

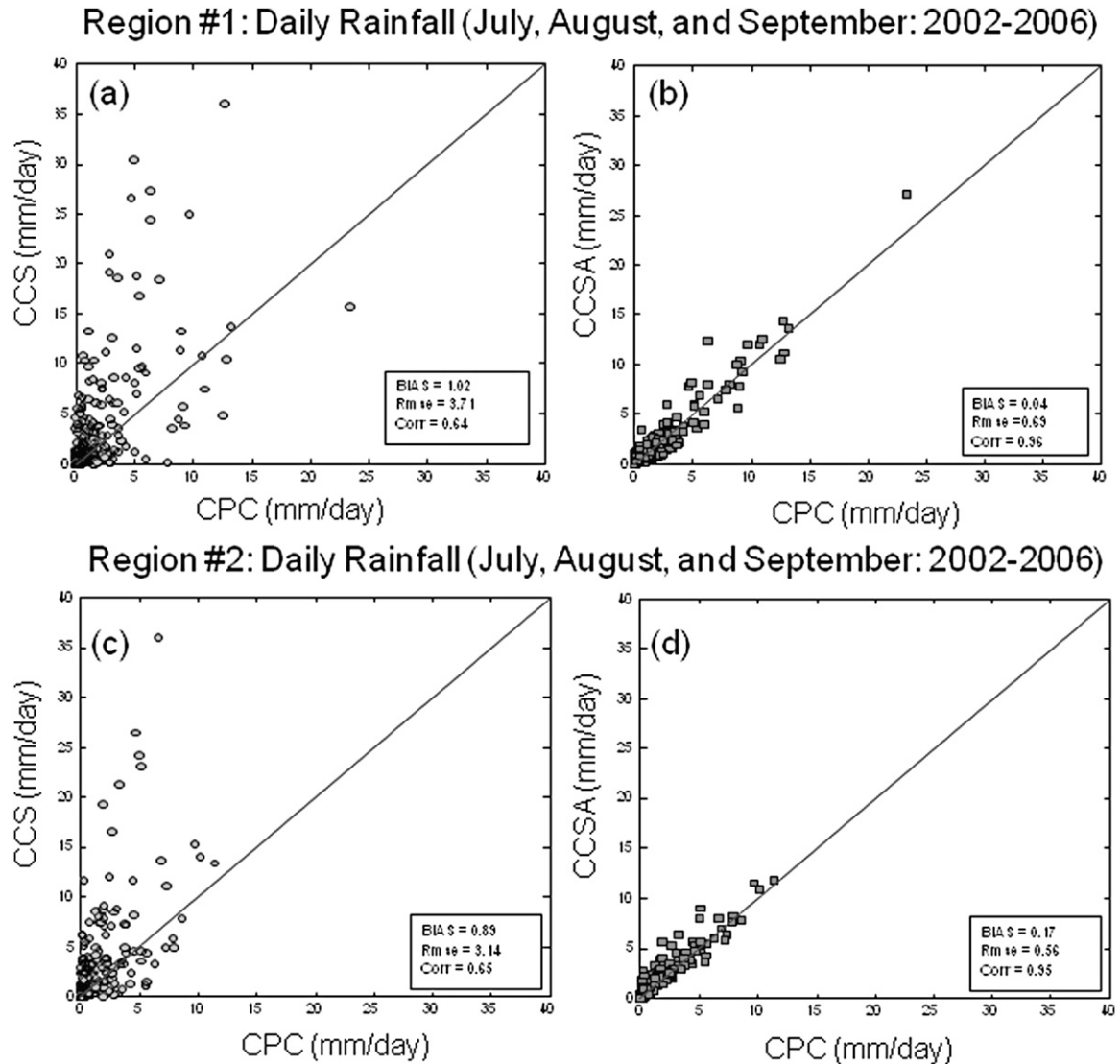## Region #2: Daily Rainfall (July, August, and September: 2002-2006)

FIG. 4. Daily intercomparison of (left) CCS and (right) CCSA against CPC gauge analysis.

effectiveness of the adjustment algorithm at finer spatial and temporal scale in the following evaluation. The original and adjusted satellite rainfall estimations described in this paper are compared to an independent rainfall observation dataset. The high-quality hourly gauge network over Walnut Gulch is used in the evaluation. The Walnut Gulch Experimental Watershed is located in southeastern Arizona (31°43′N, 110°41′W; Fig. 3b) surrounding the historical town of Tombstone. It has been used by the U.S. Department of Agriculture (USDA) as a research facility since the mid-1950s. A dense network of 88 rain gauges distributed across the watershed area that covers approximately 150 km^2 provides a good test site to evaluate the CCSA performance, given that only one gauge is listed in the CPC network

over this watershed. Historical hourly gauge precipitation of this dense network can be obtained from the Agricultural Research Service (ARS) Web site on a gauge-by-gauge basis. The watershed mean precipitation is then calculated by calculating the mean average of the quality-controlled gauge precipitation within the watershed area.

The mean monthly rainfall totals over the available period of 5-yr records (2001–05) from satellite and high gauge network measurements shows that the two summer months of July and August predominantly record most of the rainfall from both datasets (Figs. 6a–d). This figure compares the gauge measurements to the satellite estimates before and after the adjustment in which CCS estimates carry a consistent positive total bias all year long except for the month of September (see Fig. 6d).
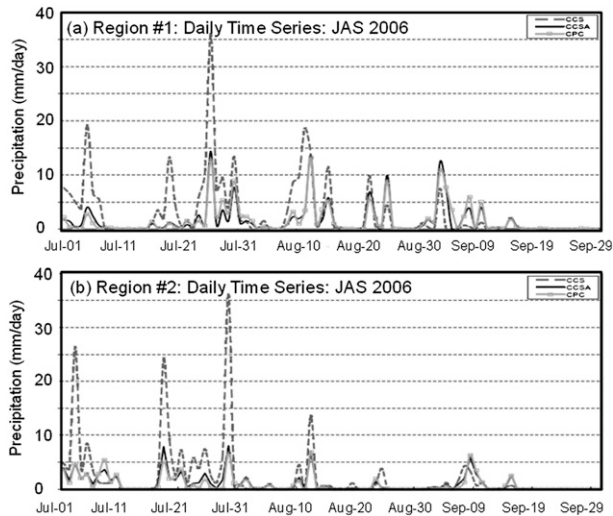
FIG. 5. Time series of the CCS, CCSA, and CPC over the $1° \times 1°$ box regions in Arizona for (top) region 1 and (bottom) region 2.

The monthly total bias is defined as the difference between the satellite mean monthly total and the gauge network mean monthly total for each month. At the same time, the CCSA shows a significant monthly total bias reduction. Furthermore, during the high-rainfall period of JA, the monthly average bias from CCS is more than 60 mm month^{-1} for each month, whereas it has been reduced by 83% (less than 10 mm month^{-1}) when the adjustment procedure is applied (see Fig. 6d).

Given that the JA period dominates the total rainfall over the southwestern U.S. region, this period has been

chosen for the high-temporal-resolution comparison for the 6-yr available records. Figure 7 depicts a sequence of scatterplots of hourly (including nonrainfall events), 3 hourly, 6 hourly, 12 hourly, and daily satellite precipitation estimations (before and after adjustment) against high gauge network measurements over Walnut Gulch. The hourly comparison shows an overestimation of CCS resulting in a CORR of 0.48, a BIAS of 0.03, and RMSE of 0.60. Statistics are consistently improved after the adjustment procedure is applied to 0.59 for the correlation, 0.00 for the bias, and 0.59 for the RMSE. Hourly rainfall from satellite measurement is mainly calculated from one or two image samples in a 1-h period. It may not represent the rainfall during the 1-h period effectively. Therefore, there is a considerable spread in this comparison of hourly rainfall by gauge and satellites.

To understand the time lag between the two sources in capturing the same event, one needs to look at the different methods in which each source is measuring the rainfall. Although the gauge network measures rainfall directly at the ground, the satellite actually estimates the rainfall amount based on the temperature and texture at the top of the cloud. The temporal aggregation of 3-, 6-, 12-, and 24-h comparison represent the same patterns in terms of the CCSA improvement over the CCS but a limited increase in terms of the overall correlation between satellite and gauge measurements. The CCSA compared to the CCS shows a bias reduction of 92%, 85%, 86%, 84%, and 84% for the 1-, 3-, 6-, and 12-hr and daily resolutions, respectively.

Further evaluation of the quantitative comparison of the hourly rainfall over Walnut Gulch is carried out by
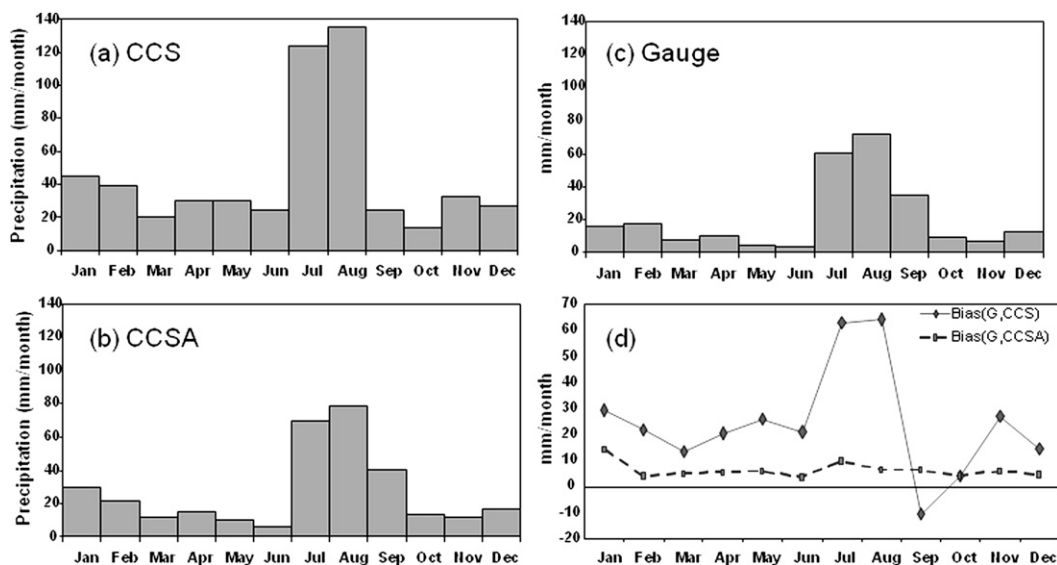

FIG. 6. Mean monthly precipitation over Walnut Gulch watershed for the period 2001–06 from different sources: (a) CCS estimates, (b) CCSA estimates, (c) gauge network measurements, and (d) monthly total bias.
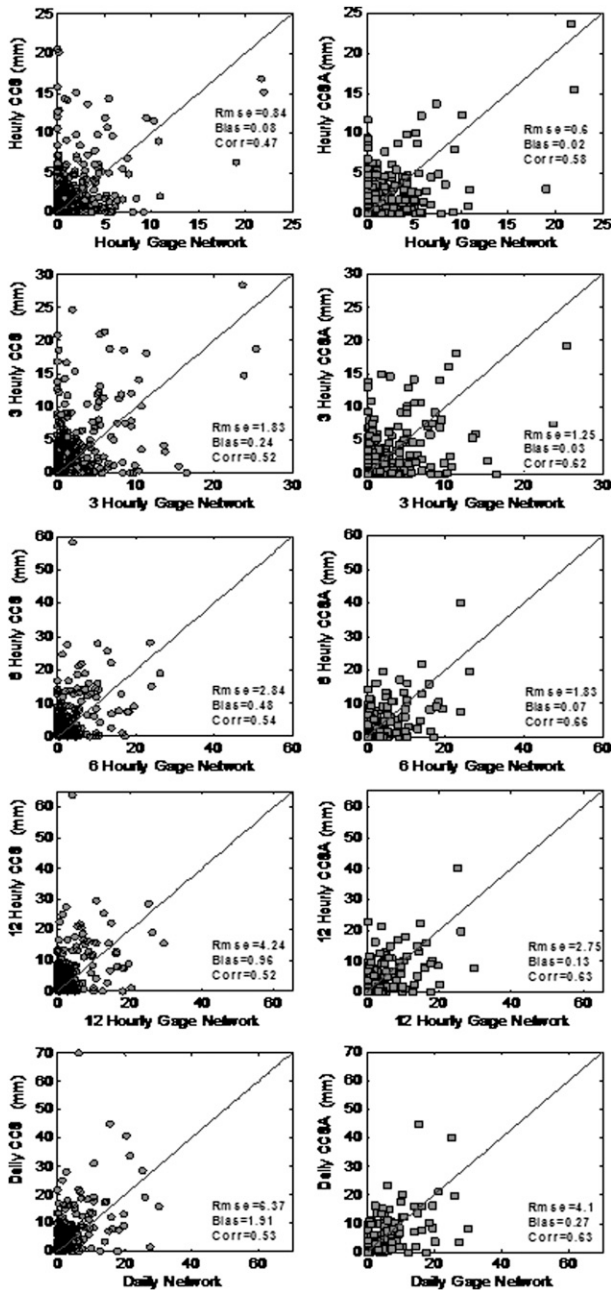
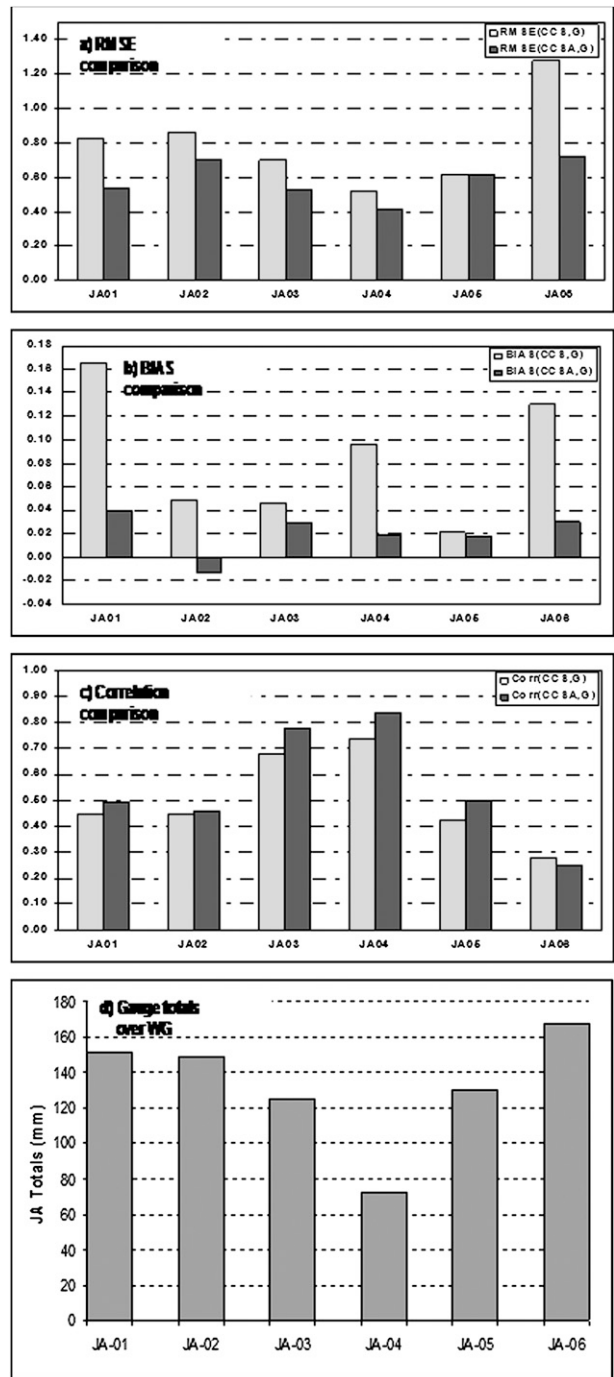FIG. 7. Scatterplots of (left) CCS and (right) CCSA vs gauge network at five temporal-scale aggregations.

FIG. 8. Statistics of hourly precipitation for the JA period of each year from 2001 to 2006: (a) RMSE, (b) BIAS, and (c) CORR (dark color represents statistics for CCSA and the light color is for CCS), and (d) total-gauge rainfall for JA periods.

calculating the statistics for each JA period of each year for the 6-yr period of record starting from 2001. Figure 8 summarizes the statistical measures for each period. The year-to-year comparison shows a reduction in the RMSE measure for all years except for 2005 after applying the bias adjustment. The BIAS measurement on the other hand shows a discerned reduction in the satellite-adjusted estimates for all years. The year-to-year comparison also shows a significant variation in the correlation measure.

Plotting the gauge-total rainfall for the JA season (Figs. 8c,d) shows that the correlation between gauge and satellite data is higher for drier years. The JA period of 2003 and 2004 shows an hourly correlation of statistical

TABLE 1. The evaluation statistics of the CCS and CCSA in rain detection under two rain thresholds (0 and 0.25 mm h^{-1}), and several accumulation time durations from 1 to 12 h.

Statistics (mm h^{-1}, h)	CCS vs gauge				CCSA vs gauge			
	BS	POD	FAR	CSI	BIAS	POD	FAR	CSI
$R > 0$, $\Delta t = 1$	1.60	0.71	0.55	0.37	1.38	0.65	0.52	0.38
$R > 0$, $\Delta t = 6$	1.37	0.85	0.37	0.56	1.24	0.81	0.34	0.57
$R > 0$, $\Delta t = 12$	1.24	0.89	0.28	0.66	1.17	0.85	0.26	0.65
$R > 0.25$, $\Delta t = 1$	1.91	0.64	0.66	0.28	1.30	0.54	0.58	0.30
$R > 0.25$, $\Delta t = 6$	1.62	0.85	0.47	0.47	1.26	0.76	0.40	0.50
$R > 0.25$, $\Delta t = 12$	1.52	0.89	0.14	0.54	1.28	0.81	0.36	0.55

significance (0.68 and 0.73) between gauge and CCS that increased about 10% when applying the bias adjustment procedure. On the other hand, years 2001, 2002, and 2005 show a correlation of less than 0.45 between gauge and CCS that benefited from a marginal gain (4%, 1%, and 7%) after applying the bias adjustment. Although the correlation over the July and August 2006 period is low (<0.3) for both CCS and CCSA with the gauge network, both the BIAS and RMSE were significantly improved. Specifically, the BIAS was reduced by 77% after applying the adjustment procedure and the RMSE was reduced by 43%. In fact, after removing the 2006 period from the previous 6-yr analysis, the CCSA hourly correlation is improved from 0.58 to 0.63, and the daily correlation is increased from 0.63 to 0.70 for the 5-yr summer period.

Table 1 shows the evaluation of CCS and CCSA to detect the nonzero rain event with accumulation of 1-, 6-, and 12-h time interval at the Walnut Gulch watershed. Four evaluation statistics were used, including bias score (BS), probability of detection (POD), false-alarm rate (FAR), and critical success index (CSI; Jolliffee and Stephenson 2003). It shows that the adjustment using CPC daily analysis improves the BS, FAR, and CSI but reduced the POD. As described in Fig. 6, the CCS consists of positive bias for around 30%–60%; the adjustment from CPC daily analysis helps to reduce the bias, which also improves the FAR and CSI. It also shows that the evaluated statistics also improved by accumulating rainfall with longer duration. Meanwhile, all the statistics get worse when the threshold level is increases from 0 to 0.25 mm h^{-1}.

c. Diurnal variation of precipitation

Figure 9 shows a comparison of the JA rainy season over Walnut Gulch during the years 2002, 2004, 2006, and the 2001–06 average from the gauge network, the CCS, and the CCSA. Although this figure shows a similar pattern of late-afternoon peak from all precipitation sources, the overestimation of rainfall by the CCS is clearly observed. The figure also shows that there is a

proportional relationship between the CCS bias and the average rainfall rate. This can be explained by the existence of a high bias of the CCS at the higher rainfall rate. A similar pattern of CCS was reported by Hong et al. (2007). In contrast, the CCSA shows a significant decrease in the bias during the high-rainfall rate cycle. On the other hand, the CCSA results in a negative bias starting from midnight to the early morning, which coincides with the decreasing rainfall-rate cycle. Evaluation statistics, as shown in Figs. 7, 9, show that improvement can be made for CCS adjustment from daily to subdaily scales using daily CPC gauge analysis. As presented in Fig. 9, the phase of the monsoon season rainfall shows it is consistent between the gauge and satellite measurements. In addition, it demonstrated that the overestimation from CCS is improved significantly using daily CPC gauge analysis. It is concluded that using CCS to downscale CPC daily analysis to subdaily scale is effective.

5. Summary and conclusions

A procedure for bias removal of satellite rainfall estimation is introduced. This procedure uses precipitation information from gauge measurement to the spatially and temporally distributed satellite-based estimation. The CPC daily analysis precipitation was used as a reference source for bias correction of the CCS satellite estimates to produce a satellite bias-adjusted estimate named CCSA. The hourly bias correction was carried out by redistributing the daily bias proportionally to the hourly rainfall estimate. The CCSA and CCS were compared to the CPC analysis product on daily basis at two selected locations in the southwestern United States and cross validated with a high-quality gauge network of precipitation at higher temporal scale over the Walnut Gulch watershed. The case studies show that the adjusted bias of CCS rainfall using daily CPC rainfall analysis was effective in reducing the bias of the PERSIANN-CCS estimates. On the subdaily scale, improvement in the RMSE and BIAS reduction is revealed; however, a limited improvement is noticed in terms of correlation.
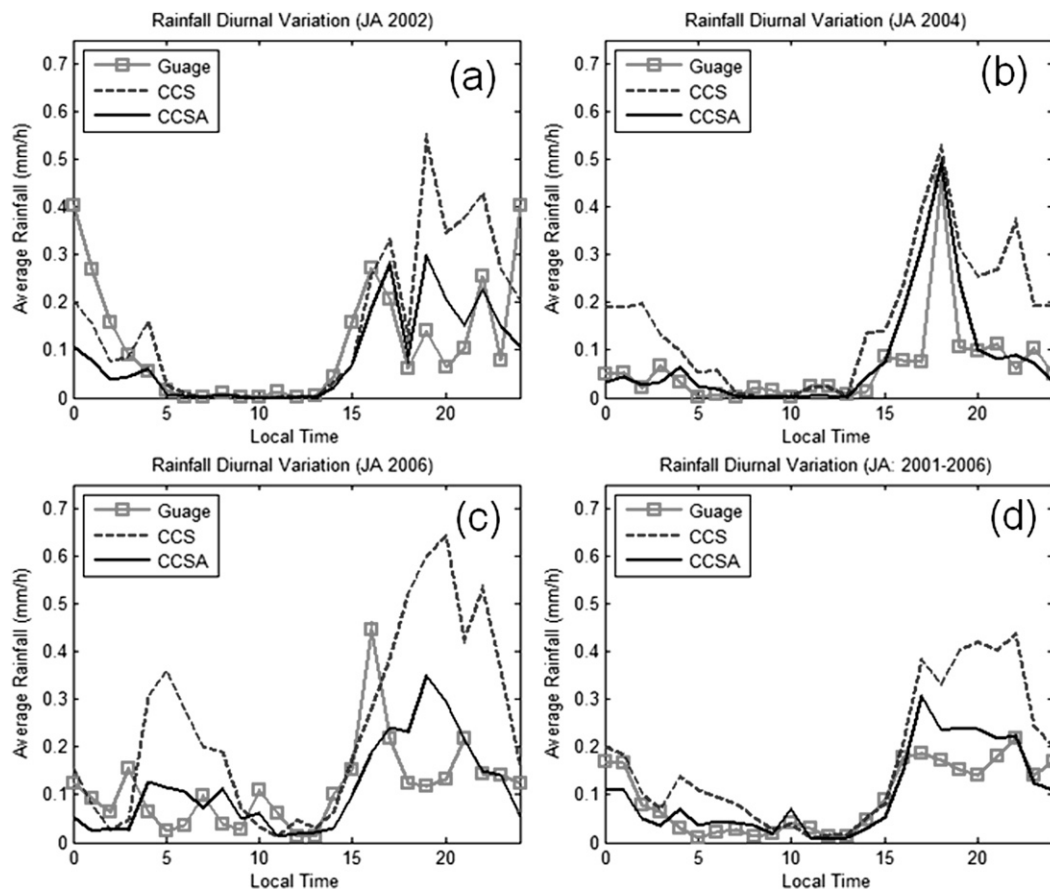
FIG. 9. Rainfall diurnal variation for the JA period of (a) 2002, (b) 2004, (c) 2006, and (d) 2001–06 average over the Walnut Gulch watershed.

In regions where the number of gauges is limited, the improvement of rainfall estimates is dependent on the quality of the satellite estimates themselves.

In conclusion, the CCSA provides an additional source of precipitation estimates that combines the strengths of ground measurement and satellite estimates at higher temporal and spatial distribution and benefits hydrologic applications, especially in areas where radar coverage is limited. Testing of the use of CCSA estimates for sub-daily scale hydrologic applications is ongoing and will be discussed in the future reports.

REFERENCES

Adler, R. F., J. A. Negri, P. R. Keehn, and I. M. Hakkarinen, 1993: Estimation of monthly rainfall over Japan and surrounding waters from a combination of low-orbit microwave and geo-synchronous IR data. *J. Appl. Meteor.,* **32,** 335–356.

——, G. J. Huffman, D. T. Bolvin, S. Curtis, and E. J. Nelkin, 2000: Tropical rainfall distributions determined using TRMM combined with other satellite and rain gauge information. *J. Appl. Meteor.,* **39,** 2007–2023.

Ba, M. B., and A. Gruber, 2001: GOES multispectral rainfall algorithm (GMSRA). *J. Appl. Meteor.,* **40,** 1500–1514.

Battan, L. J., 1973: *Radar Observation of the Atmosphere.* University of Chicago Press, 324 pp.

Bellerby, T., M. Todd, D. Kniveton, and C. Kidd, 2000: Rainfall estimation from a combination of TRMM precipitation radar and GOES multispectral satellite imagery through the use of an artificial neural network. *J. Appl. Meteor.,* **39,** 2115–2128.

Bowman, K. P., A. B. Phillips, and G. R. North, 2003: Comparison of TRMM rainfall retrievals with rain gauge data from the TAO/TRITON buoy array. *Geophys. Res. Lett.,* **30,** 1757, doi:10.1029/2003GL017552.

Daley, R., 1991: *Atmospheric Data Analysis.* Cambridge University Press, 457 pp.

Droegemeier, K. K., and Coauthors, 2000: Hydrological aspects of weather prediction and flood warnings: Report of the Ninth Prospectus Development Team of the U.S. Weather Research Program. *Bull. Amer. Meteor. Soc.,* **81,** 2665–2680.

Gandin, L. S., 1963: *Objective Analysis of Meteorological Fields* (in Russian). Gidrometeorologicheskoe Izdate'stvo, 286 pp.

Gochis, D. J., L. Brito-Castillo, and W. J. Shuttleworth, 2006: Hydroclimatology of the North American Monsoon region in Northwest Mexico. *J. Hydrol.,* **316,** 53–70.

Groisman, P. Ya., and D. R. Easterling, 1994: Variability and trends of total precipitation and snowfall over the United States and Canada. *J. Climate,* **7,** 184–205.

Gruber, A., X. Su, M. Kanamitsu, and J. Schemm, 2000: The comparison of two merged rain gauge satellite precipitation datasets. *Bull. Amer. Meteor. Soc.,* **81,** 2631–2644.

Higgins, R. W., W. Shi, E. Yarosh, and R. Joyce, 2000: Improved United States precipitation quality control system and analysis. *NCEP/Climate Prediction Center Atlas 7,* 40 pp.

Hong, Y., K. L. Hsu, S. Sorooshian, and X. Gao, 2004: Precipitation estimation from remotely sensed information using an artificial neural network-cloud classification systems. *J. Appl. Meteor.,* **43,** 1834–1852.

——, D. Gochis, J. Cheng, K.-L. Hsu, and S. Sorooshian, 2007: Evaluation of PERSIANN-CCS rainfall measurement using the NAME Event Rain Gauge Network. *J. Hydrometeor.,* **8,** 469–482.

Hsu, K., X. Gao, S. Sorooshian, and H. V. Gupta, 1997: Precipitation estimation from remotely sensed information using artificial neural networks. *J. Appl. Meteor.,* **36,** 1176–1190.

——, H. V. Gupta, X. Gao, and S. Sorooshian, 1999: Estimation of physical variables from multi-channel remotely sensed imagery using a neural network: Application to rainfall estimation. *Water Resour. Res.,* **35,** 1605–1618.

Huff, F. A., 1970: Sampling errors in measurement of mean precipitation. *J. Appl. Meteor.,* **9,** 35–44.

Huffman, G. J., 1997: Estimates of root-mean-square random error for finite samples of estimated precipitation. *J. Appl. Meteor.,* **36,** 1191–1201.

——, R. F. Adler, M. Morrissey, D. T. Bolvin, S. Curtis, R. Joyce, B. McGavock, and J. Susskind, 2001: Global precipitation at one-degree daily resolution from multisatellite observations. *J. Hydrometeor.,* **2,** 36–50.

Jolliffe, I. T., and D. B. Stephenson, 2003: *Forecast Verification: A Practitioner's Guide in Atmospheric Science.* Wiley and Sons, 254 pp.

Joyce, R. J., J. E. Janowiak, P. A. Arkin, and P. Xie, 2004: CMORPH: A method that produces global precipitation estimates from passive microwave and infrared data at high spatial and temporal resolution. *J. Hydrometeor.,* **5,** 487–503.

Kummerow, C., W. Barnes, T. Kozu, J. Shiue, and J. Simpson, 1998: The Tropical Rainfall Measuring Mission (TRMM) sensor package. *J. Atmos. Oceanic Technol.,* **15,** 809–817.

Legates, D. R., 1993: Biases in precipitation gauge measurements. Global observations, analysis and simulation of precipitation, World Climate Programme Research Rep. WCRP-78, 31–34.

Levizzani, V., P. Bauer, and F. J. Turk, 2007: *Measuring Precipitation from Space: EURAINSAT and the Future.* Advances in Global Change Research, Vol. 28, Springer, 722 pp.

Marshall, J. S., and W. M. Palmer, 1948: The distribution of raindrops with size. *J. Meteor.,* **5,** 165–166.

Marzano, F. S., M. Palmacci, D. Cimino, G. Giuliano, and F. J. Turk, 2004: Multivariate statistical integration of satellite infrared and microwave radiometric measurements for rainfall retrieval at the geostationary scale. *IEEE Trans. Geosci. Remote Sens.,* **42,** 1018–1032.

McCollum, J. R., A. Gruber, and M. B. Ba, 2000: Discrepancy between gauges and satellite estimates of rainfall in equatorial Africa. *J. Appl. Meteor.,* **39,** 666–679.

——, W. F. Krajewski, R. R. Ferraro, and M. B. Ba, 2002: Evaluation of biases of satellite rainfall estimation algorithms over the continental United States. *J. Appl. Meteor.,* **41,** 1065–1080.

Morin, E., R. A. Maddox, D. C. Goodrich, and S. Sorooshian, 2005: Radar *Z–R* relationship for summer monsoon storms in Arizona. *Wea. Forecasting,* **20,** 672–679.

Morrissey, M., 1991: Using sparse rain gauges to test satellite-based rainfall algorithm. *J. Geophys. Res.,* **96,** 18 561–18 571.

Reynolds, R. W., and T. M. Smith, 1994: Improved global sea surface temperature analyses using optimum interpolation. *J. Climate,* **7,** 929–948.

Rosenfeld, D., and Y. Mintz, 1988: Evaporation of rain falling from convective clouds as derived from radar measurements. *J. Appl. Meteor.,* **27,** 209–215.

Scofield, R. A., and V. J. Oliver, 1977: A scheme for estimating convective rainfall from satellite imagery. NOAA Tech. Memo. NESS 86, U.S. Department of Commerce, 47 pp.

Sevruk, B., 1985: Correction of precipitation measurements: Summary report. *Proc. Workshop on the Correction of Precipitation Measurements,* Zurich, Switzerland, World Meteorological Organization, 13–23.

Smith, J. A., and W. F. Krajewski, 1991: Estimation of the mean field bias of radar rainfall estimates. *J. Appl. Meteor.,* **30,** 397–412.

Smith, T. M., P. A. Arkin, J. J. Bates, and G. J. Huffman, 2006: Estimating bias of satellite-based precipitation estimates. *J. Hydrometeor.,* **7,** 841–856.

Sorooshian, S., K.-L. Hsu, X. Gao, H. Gupta, B. Imam, and D. Braithwaite, 2000: Evaluation of PERSIANN system satellite-based estimates of tropical rainfall. *Bull. Amer. Meteor. Soc.,* **81,** 2035–2046.

Tapiador, F. J., C. Kidd, K.-L. Hsu, and F. S. Marzano, 2004: Neural networks in satellite rainfall estimation. *Meteor. Appl.,* **11,** 83–91.

Turk, F. J., G. Rohaly, J. D. Hawkins, E. A. Smith, A. Grose, F. S. Marzano, A. Mugnai, and V. Levizzani, 2000: Analysis and assimilation of rainfall from blended SSM/I, TRMM and geostationary satellite data. *Proc. 10th Conf. on Satellite Meteorology and Oceanography,* Long Beach, CA, Amer. Meteor. Soc., 2.2. [Available online at http://ams.confex.com/ams/annual2000/techprogram/paper_147.htm.]

Vicente, G. A., R. A. Scofield, and W. P. Menzel, 1998: The operational GOES infrared rainfall estimation technique. *Bull. Amer. Meteor. Soc.,* **79,** 1883–1898.

Willmott, C. J., and K. Matsuura, 1995: Smart interpolation of annually averaged air temperature in the United States. *J. Appl. Meteor.,* **34,** 2577–2586.

Wilson, J. W., and E. A. Brandes, 1979: Radar measurement of rainfall—A summary. *Bull. Amer. Meteor. Soc.,* **60,** 1048–1058.

Xie, P., and P. A. Arkin, 1997: Global precipitation: A 17-year monthly analysis based on gauge observations, satellite estimates, and numerical model outputs. *Bull. Amer. Meteor. Soc.,* **78,** 2539–2558.

Yilmaz, K. K., T. S. Hogue, K.-L. Hsu, S. Sorooshian, H. V. Gupta, and T. Wagener, 2005: Intercomparison of rain gauge, radar, and satellite-based precipitation estimates with emphasis on hydrologic forecasting. *J. Hydrometeor.,* **6,** 497–517.